Carbohydrate Polymers 87 (2012) 1495–1502

Contents lists available at SciVerse ScienceDirect

Carbohydrate Polymers

journal homepage: www.elsevier.com/locate/carbpol

Carboxymethylcellulose–montmorillonite nanocomposite films activated with murta (*Ugni molinae* Turcz) leaves extract

Marcela Quilaqueo Gutiérrez[a], Ignacio Echeverría[b], Mónica Ihl[a,c], Valerio Bifani[c], Adriana N. Mauri[b,*]

[a] *Fundación de Desarrollo Educacional y Tecnológico La Araucanía (FUDEAUFRO), Montevideo 780, Temuco, Chile*
[b] *Centro de Investigación y Desarrollo en Criotecnología de Alimentos (CIDCA, CCT – La Plata, CONICET and Facultad de Ciencias Exactas, Universidad Nacional de La Plata), Calle 47 y 116 S/N, B1900AJJ La Plata, Buenos Aires, Argentina*
[c] *Department of Chemical Engineering, Universidad de La Frontera, P.O. Box 54D, Temuco, Chile*

ARTICLE INFO

Article history:
Received 3 August 2011
Received in revised form 9 September 2011
Accepted 12 September 2011
Available online 17 September 2011

Keywords:
Carboxymethylcellulose
Murta leaves extracts
Montmorillonite
Nanocomposites active films
Antioxidant properties

ABSTRACT

The functionality of nanocomposite films based on carboxymethylcellulose (CMC) and montmorillonite (MMT) activated with murta (*Ugni molinae* Turcz) leaves extract was studied. Films were prepared by casting from film-forming dispersions containing CMC, glycerol (used as plasticizer) and different concentrations of MMT, using water or murta extract as solvent. The addition of MMT increased the tensile strength and the elasticity modulus of the films, and decreased their permeabilities to water vapor, oxygen and carbon dioxide. Besides the antioxidants properties provided to the films, the addition of murta leaves extract changed the gas permeability in different forms according to the MMT content, and plasticized the nanocomposite matrix.

1. Introduction

The use of biopolymers as substitutes for non-degradable synthetic polymers is considered a sustainable alternative, particularly interesting for short-term applications, such as food packaging. Among the biopolymers, anionic linear polysaccharides derived from cellulose, as methylcellulose and the carboxymethylcellulose (CMC), have excellent film-making properties, large availability, low cost, and easy processability. Films prepared with these polymers generally have good gas barrier properties and moderate to good mechanical properties, but they are very susceptible to moisture (Bifani et al., 2007; Rimdusit, Sorada, Siriporn, & Sunan, 2008).

Currently, one of the most effective alternatives to improve the barrier and mechanical properties of packaging materials, either synthetic or natural, is the formation of nanocomposites. Among all the potential nanocomposite precursors, those based on layered silicates have been more widely investigated probably because the starting clay materials are easily available and environmentally friendly, have low cost, and their intercalation chemistry has been studied for a long time (Alexandre & Dubois, 2000; Ogawa & Kuroda, 1997). Montmorillonite (MMT) is the most commonly used layered silicate. Its crystal lattice consists of 1 nm thin layers formed by an octahedral alumina sheet sandwiched between two tetrahedral silica sheets. It has a high surface area (aspect ratio of about 100), and is negatively charged (Sinha Ray & Okamoto, 2003). The stacking of these layers leads to a Van der Waals gap or gallery, in which alkaline cations, such as Na^+, Li^+ or Ca^{2+}, are located and neutralize the charge. The major problem in preparing these composites is to separate the initially agglomerated clay layers, which is a necessary step because polymer properties are improved when the clay layers are well dispersed in the polymer matrix (Alexandre & Dubois, 2000; Giannelis, 1996; Sinha Ray & Bousmina, 2005). Thus, it has been possible to improve the properties of polysaccharide films, mainly based on starch and methylcellulose, by the addition of small amounts ($\leq$10%) of MMT (Almasi, Ghanbarzadeh, & Entezami, 2010; Cyras, Manfredi, Ton-That, & Vazquez, 2008; Dean, Yu, & Wu, 2007; Rimdusit et al., 2008; Tang, Alavi, & Herald, 2008).

Another strategy to improve the functionality of the applicable materials in packaging is to activate them with various types of additives such as antioxidants, antimicrobials, vitamins, flavors, and colorants to improve their appearance, and to extend the shelf-life of the food they protect (Gómez Estaca, Giménez, Gómez-Guillén, & Montero, 2009; Han & Krochta, 2007). Currently there is a preference for the use of natural active compounds instead of synthetic ones, such as plant extracts, for food preservation. Tea prepared from leaves of murta or murtilla (*Ugni molinae* Turcz), a native plant of the South of Chile, was highly valued as a folk medicine by the Chilean Mapuche aborigines. For its physiological benefits, mainly a kidney-protective effect (Montenegro, 2002; Seguel, Peñalosa, Gaete, Montenegro, & Torres, 2000). Nowadays it

* Corresponding author.
E-mail address: anmauri@quimica.unlp.edu.ar (A.N. Mauri).

0144-8617/$ – see front matter © 2011 Elsevier Ltd. All rights reserved.
doi:10.1016/j.carbpol.2011.09.040

is known that the alcoholic and water extracts of the leaves contain high levels of polyphenols and posses antioxidant properties (Rubilar et al., 2006). Bifani et al. (2007) used the aqueous extracts of two different ecotypes of murta leaves for the preparation of edible films of carboxymethylcellulose with distinguished barrier properties to water vapour, CO_2 and O_2, because of different quantities of the flavonols myricetin and quercetin found in both ecotypes. Gomez-Guillén, Ihl, Bifani, Silva, and Montero (2007) observed that the addition of murta leaves extracts to tuna fish (*Thunnus tynnus*) gelatin-based films led to transparent films with increased protection against UV light as well as antioxidant capacity and modified physical properties.

The potential utilization of a polymer/layered silicate system as carrier or vehicle for active compounds in the field of active food packaging is currently being explored. Mascheroni, Chalier, Gontard, and Gastaldi (2010) developed a delivery system for carvacrol based on a wheat gluten matrix reinforced with MMT fillers (≥5%) that was clearly efficient to retain and protect the antimicrobially active agent during the processing stage.

The aim of this study was to evaluate the functionality of CMC–MMT nanocomposite films activated with murta leaves extract.

2. Materials and methods

2.1. Materials

Fresh leaves of murta (*U. molinae* Turcz) of Casa ecotype were sampled in Temuco, Chile. Sodium carboxymethylcellulose (CMC), molecular weight (MW) 280–400 kDa, degree of substitution (DS) 07–09, was purchased from Prinal S.A. (Santiago, Chile). Sodium montmorillonite without organic modification (MMT, Cloisite®Na^+) was supplied by Southern Clay Products (USA). It has a cation exchange capacity (CEC) of 92.6 meq/100 g clay, a typical interlayer distance of 11.7 Å, a bulk density of 2.86 g cm^{-3} and a typical particle size distribution between 2 and 13 μm.

2.2. Obtaining murta leaves extract

Leaves samples were air-dried in an oven (Memmert Cientec) at 25 °C until they reached a moisture content of 4.65%. Subsequently the leaves were milled in a coffee grinder. Dried and milled murta leaves were extracted at 25 °C for 90 min with distilled water (75 mg/mL) in an Erlenmeyer flask placed in a shaking incubator at 170 rpm. Then the mixture was filtered under vacuum to obtain the water extract.

2.3. Preparation of films

On one hand, 2 g of CMC was dispersed in 80 mL of distilled water or murta leaves extract under magnetic stirring at room temperature. On the other hand, different concentrations of MMT were dispersed in 20 mL of distilled water with magnetic stirring for 20 min at room temperature, followed by sonication using an ultrasound equipment (Sonics Vibra-cell model VCX 750; Sonics & Materials, Inc, USA) for 1 min and 80% amplitude. Finally, CMC and clay dispersions were mixed at 170 rpm, for 24 h at 25 °C. Each film-forming dispersion (13 g) was poured on polystyrene Petri dishes (64 cm^2) and then dehydrated at 60 °C for 4 h in an oven with air flow circulation (Yamato, DKN600, USA). Dry films with 0, 5, and 10 g of MMT per 100 g of CMC, activated or not with the active compounds of the murta extract leaves, were obtained and conditioned 48 h at 20 °C and 58% relative humidity (RH) in desiccators with saturated solutions of NaBr, before being peeled from the casting surface for characterization.

2.4. Film thickness

Film thickness was measured by a digital coating thickness gauge (Check Line DCN-900, USA). Measurements for testing mechanical properties, and oxygen and water barrier properties were performed at nine different locations on the films. The mean thickness was used to calculate these physical properties.

2.5. Moisture content (MC)

MC was determined after drying in an oven at 105 °C for 24 h. Small specimens of films (≈0.25 g) collected after conditioning, were cut and placed on aluminum containers that were weighed before and after oven drying. MC values were determined in triplicate for each film, and calculated as the percentage of weight loss based on the original weight (ASTM D644-94, 1994).

2.6. Color

Films color was determined using a Minolta Chroma meter (CR 300, Minolta Chroma Co., Osaka, Japan). A CIE Lab color scale was used to measure the degree of lightness (L), redness ($+a$) or greenness ($-a$), and yellowness ($+b$) or blueness ($-b$) of the films. The instrument was standardized using a set of three Minolta calibration plates. Films were measured on the surface of the white standard plate with color coordinates of $L_{standard} = 97.3$, $a_{standard} = 0.14$ and $b_{standard} = 1.71$. Total color difference (ΔE) was calculated from:

$$\Delta E = \sqrt{(L_{film} - L_{standard})^2 + (a_{film} - a_{standard})^2 + (b_{film} - b_{standard})^2} \quad (1)$$

values were expressed as the means of nine measurements on different areas of each film.

2.7. X-ray diffraction (XRD)

XRD analyses of the films were performed in a Bruker X'Pert diffractometer (PANalytical, USA) equipped with a Cu Kα radiation source ($\lambda = 0.154$ nm). The voltage and the current used were 40 kV and 40 mA, respectively. The diffraction data were collected from $2\theta = 1.5–10°$ in a fixed time mode with a step interval of 0.01°.

2.8. Water vapor permeability (WVP)

Water vapor permeability tests were conducted using ASTM method E 96-80 (1989) with some modifications (Gennadios, McHugh, Weller, & Krochta, 1994). Each film sample was sealed over a circular opening of 0.00185 m^2 in a permeation cell that was stored at 20 °C in a desiccator. To maintain a 75% relative humidity (RH) gradient across the film, anhydrous silica (0% RH_c) was placed inside the cell and a saturated NaCl solution (75% RH_d) was used in the desiccator. The RH inside the cell was always lower than outside, and water vapor transport was determined from the weight gain of the permeation cell. When steady-state conditions were reached (about 1 h), eight weight measurements were made over 7 h. Changes in the weight of the cell were recorded and plotted as a function of time. The slope of each line was calculated by linear regression (Origin Pro 8.5) and the water vapor transmission rate (WVTR) was calculated from the slope (g H_2O/s) divided by the cell area (m^2). WVP (g H_2O/(Pa s m)) was calculated as:

$$WVP = \frac{WVTR}{P_v^{H_2O}(RH_d - RH_c)A} d \quad (2)$$

where $P_v^{H_2O}$ = vapor pressure of water at saturation (1753.35 Pa) at the test temperature (20 °C), $RH_d = RH$ in the desiccator, $RH_c = RH$

in the permeation cell, A = permeation area, and d = film thickness (m). Each WVP value represents the mean value of at least three samples taken from different films.

2.9. Gas permeability measurements

Oxygen and carbon dioxide permeability of the films were assessed by the accumulation method (Bifani et al., 2007; García, Martino, & Zaritzky, 2000), in a specially designed stainless-steel cell formed by two chambers of 89.10 cm^3 volume, separated by the film to be tested, with a transmission area of 0.0012 m^2. Gas permeability determinations were done by placing the test film between these chambers after closing the cell tightly. The total pressure difference across the film was zero and the partial pressure difference for the gas was approximately 1 atm. The quasi-isostatic method used was based on the measurement of the amount of gas diffusing through the film. To measure this concentration, 100 μL O_2 or 50 μL CO_2 gas samples were withdrawn with a Pressure-Lok® syringe (SUPELCO USA) from the test chamber, initially filled with air. Gas concentration was measured in a Clarus 500 (PerkinElmer) gas chromatograph with thermal conductivity detector with Carboxen 1000 column for oxygen permeability, and flame ionization detector with Carboxen 1006 column for carbon dioxide. Gas permeability of films was calculated and expressed in $cm^3\ m^{-1}\ s^{-1}\ Pa^{-1}$ at 25 °C and 100% RH.

2.10. Mechanical properties

The tensile strength, Young's modulus and elongation at break of the films were determined following the procedures outlined in the ASTM methods (ASTM D882-91, 1991), taking an average of six measurements for each film and using at least two films per formulation. The films were cut into 6 mm wide and 80 mm long strips, which were mounted between the grips of the texture analyzer TA.XT2i (Stable Micro Systems, Surrey, England). The initial grip separation was set at 50 mm and the crosshead speed at 0.5 mm/s. The tensile strength (σ = force/initial cross-sectional area) and elongation at break (ε) were determined directly from the stress-strain curves using Texture Expert V.1.15 software (Stable Micro Systems, Surrey, England), and the Young's modulus (E) was calculated as the slope of the initial linear portion of this curve.

2.11. Antioxidant capacity

The $ABTS^{\bullet+}$ radical (2,2-azinobis-(3-ethylbenzothiazoline-6-sulfonic acid)) scavenging capacity of the samples was determined according to a modified version of the method of Re et al. (1999). The stock solution of $ABTS^{\bullet+}$ radical consisted of 7 mM ABTS (Sigma Chemical Co. St. Louis, MO) in 2.45 mM potassium persulfate (Anedra, Argentine), kept in the dark at room temperature for 12–16 h. An aliquot of the stock solution was diluted with distilled water in order to prepare the working solution of $ABTS^{\bullet+}$ radical with an absorbance of 0.70 ± 0.03 at 734 nm. Samples of films (5 mg/50 μL of sodium phosphate buffer, pH 7.4) were added to 950 μL of the solution containing the diluted $ABTS^{\bullet+}$. The mixture was vortexed for 2 min, centrifuged for 3 min (9000 × g) (Beckman GS-15) and its absorbance at 734 nm (Abs_s) was measured 6 min after the addition of the $ABTS^{\bullet+}$ solution. To obtain a reaction blank (Abs_{rb}) in each assay, the same procedure was carried out but replacing the sample with 25 μL of sodium phosphate buffer. The antioxidant capacity (AC), as measured by the ability to scavenge the $ABTS^{\bullet+}$ radical, was calculated with Eq. (3). All determinations were performed at least in triplicate.

$$AC = \frac{Abs_{rb} - Abs_s}{Abs_{rb}} \times 100 \quad (3)$$

Table 1
Moisture content and contact angle of CMC films reinforced with montmorillonite and/or activated with murta leaves extract.

Film	Moisture content (%)	Contact angle
With water		
0 g MMT/100 g CMC	23.20 ± 0.21[b]	45.37 ± 1.87[b]
5 g MMT/100 g CMC	19.65 ± 0.37[a]	38.21 ± 1.78[a]
10 g MMT/100 g CMC	20.52 ± 0.33[a]	36.53 ± 0.84[a]
With murta extract		
0 g MMT/100 g CMC	29.26 ± 0.08[c]	48.57 ± 1.54[b]
5 g MMT/100 g CMC	20.22 ± 0.55[a]	58.35 ± 1.73[c]
10 g MMT/100 g CMC	20.13 ± 0.05[a]	67.63 ± 2.07[d]

Reported values for each films are means ± standard deviation. Values means by the same letter in column are not significantly different ($p < 0.05$) according to Tukey's test.

2.12. Contact angle

Surface hydrophobicity of films was assessed by measuring the dynamic contact angle in an environment with controlled humidity of 58% HR, using a goniometer (Model 500, ramé-hart instrument co., USA). 5 μL drop of demineralised water was placed on the surface of the film with an automatic piston syringe and photographed. An image analyzer (DROPimage Advanced v2.2) was used to measure the angle formed between the base, composed of the surface of the film in contact with the drop of water, and the tangent to the drop of water. For each film, the hydrophobicity was obtained from the values of initial contact angle (average value of contact angles measured on both sides of the drop, almost immediately after the deposition of the water drop on the film). The experimental results were the average values of five measurements made on different areas of the film surface.

2.13. Statistical analysis

Results were expressed as mean ± standard deviation and were analyzed by analysis of variance (ANOVA). Means were tested with the Tukey's HSD (honestly significant difference) test for paired comparison, with a significance level $\alpha = 0.05$, using the IBM® SPSS® Statistics version 11.0 software (IBM Corporation, USA).

3. Results and discussion

3.1. Moisture susceptibility

Table 1 shows the water content of the CMC films. Films prepared from dispersions of this biopolymer in aqueous murta extract showed significantly higher water content ($p < 0.5$) than those prepared from CMC dispersions in water. The addition of MMT decreased the water content of films formed, independently of the MMT content and the solvent used, but this diminution was significantly higher when murta leaves extract was used as solvent. Other authors (Almasi et al., 2010; Cyras et al., 2008; Huang, Yu, & Ma, 2004) observed that the moisture absorption capacity of starch or starch–CMC biocomposites was higher than that of their MMT-bionanocomposites, and they attributed this difference to the capacity of starch and CMC to form hydrogen bonds with the hydroxyl groups of the MMT layers. Huang et al. (2004) confirmed the formation of these hydrogen bonds through Fourier Transform infrared studies (FT-IR) in montmorillonite-reinforced thermoplastic starch composites. Therefore, the possible

hydrophilic interactions between CMC and MMT should lead to the formation of a strong matrix structure in which water molecules find a lower availability of hydrophilic sites, what could explain the lower water content of nanocomposite films. The fact that the murta extract does not show the same effect on CMC films in nanocomposite systems, could be an indication that most of the water absorption comes from the crosslinking network of these compounds with the CMC, and that the active compounds of the extract virtually do not contribute to water absorption into the system. And, obviously, the participation of these compounds is different in the presence of clay.

Table 1 also shows the contact angles measured when a drop of water is deposited on the film surface. The contact angle of the CMC–murta films seems to be higher than the corresponding to CMC films formed from aqueous dispersions, denoting that the presence of the plant extract produces films with more hydrophobic surfaces, despite having higher water content. The increase of surface hydrophobicity and water measurement rates, that seem contradictory results, has been previously reported (Karbowiak, Debeaufort, Champion, & Voilley, 2006; Tunc et al., 2007), indicating that static and dynamic wetting properties are not necessarily related. On the other hand, two inverse behaviors are observed when MMT is added to aqueous or murta extract systems based on CMC. When clay was added to aqueous formulations, the contact angles of the respective films decreased, implying an increase of the hydrophilic character of those surfaces. Tunc et al. (2007) observed the same behavior when adding MMT to gluten films. Cyras et al. (2008), although using different solvents as reference during contact angle evaluation, also reported an increment in the polar component of the surface energy of starch films with the addition of MMT, which was attributed to the hydrophilic character of the MMT hydroxylated silicate layer as well as to the surface morphology of the films. But when clay was added to the CMC–murta system, the contact angle increased with the MMT content, showing a higher surface hydrophobicity of these films. These results suggest that the important surface behavior of compounds present in the extract becomes even more important as clay concentration increases in the formulation, so that it would even mask the effect of the clay on surface hydrophobicity. These observations reinforce the idea that the active compounds of the extract possibly compete with reactive groups of clay for interacting with CMC.

3.2. Barrier properties

The barrier properties of the studied films are shown in Fig. 1. The addition of MMT to CMC films obtained from aqueous dispersions decreased significantly the permeability to water vapor (Fig. 1a), oxygen (Fig. 1b) and carbon dioxide (Fig. 1c), at least 54, 84 and 55% respectively, without significant differences in this effect between the different MMT concentrations.

Permeability is known to be governed by two mechanisms: diffusion and sorption. Considering the diffusional effect, the potential for enhanced barrier performance of the nanocomposite films relative to the plain films can be attributed to the large aspect ratio and surface area of the clay. That is, when dispersed sufficiently, these platelets may form a 'tortuous pathway' that gas and water molecules must follow to permeate through the film. The tortuous path theory is based on the premise that a molecule must follow a more complicated path when MMT is dispersed throughout the polymer matrix than when the matrix consists of the polymer alone. On the other hand, the possible establishment of hydrogen bonds between OH groups of CMC and nanoclays would result in a denser polymer matrix that affects the solubility of the molecules in the matrices, and thus the permeability. In particular, the water vapor molecules would be less available to the hydrophilic sites.

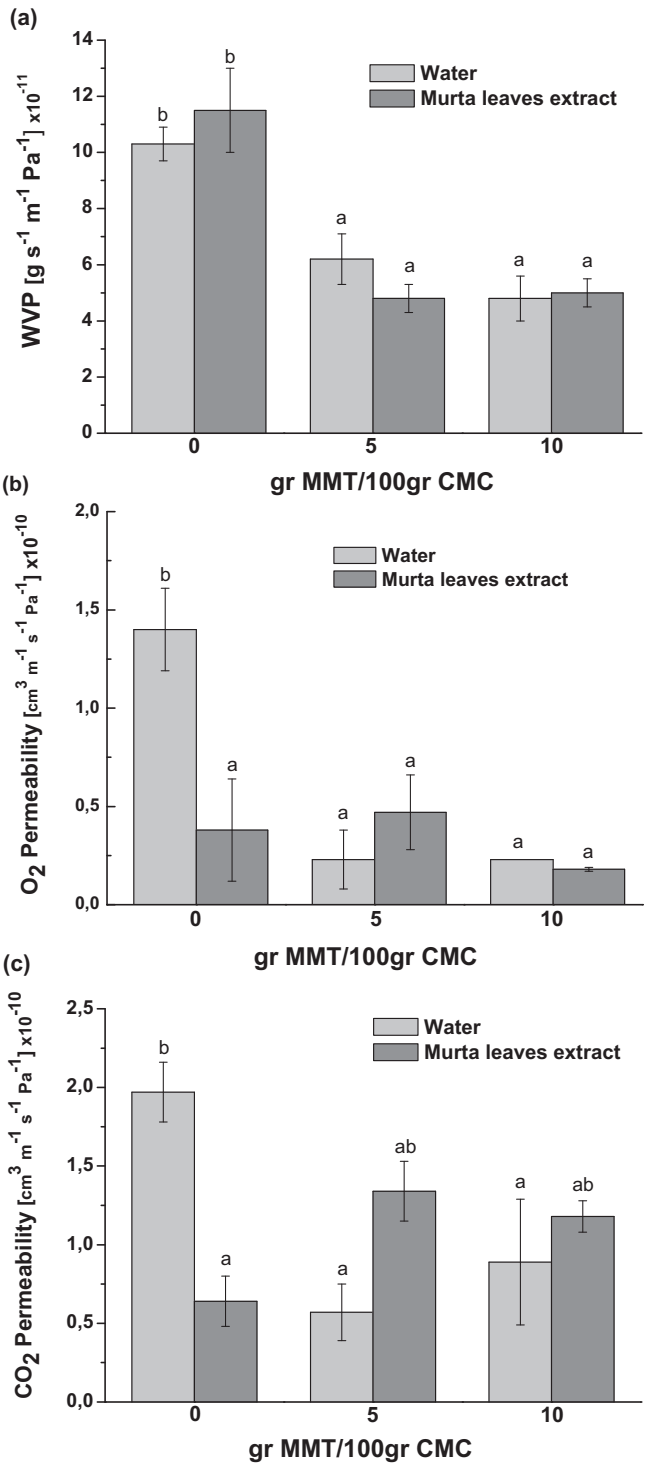

Fig. 1. Barrier properties to water-vapor (a), oxygen (b) and carbon dioxide (c) of CMC films reinforced with montmorillonite and/or activated with murta leaves' extract.

On the other hand, the films of CMC and CMC–MMT formed from dispersions in murta extract presented a WVP similar to that of the respective water-based films (Fig. 1a). Bifani et al. (2007) did not observe changes in the WVP of CMC films activated with an extract of murta of the Soloyo Chico ecotype, but found a reduced WVP when the Soloyo Grande ecotype was used, and attributed these differences to the differential composition of flavonoids and other phenolic compounds in extracts of these ecotypes. Preliminary studies (not yet published) have shown that the Casa ecotype

has a lower flavonoid content and a lower myricetin/quercetin flavonoids ratio than Soloyo Grande and Soloyo Chico ecotypes. Taking into account that myricetin shows hydroxylation in the 3′,4′,5′ positions of the B ring of the flavonol and quercetin is hydroxylated in the 3′,4′ positions, and that these OH groups may form hydrogen linkages between flavonols and CMC or MMT, it is expected that the ecotype used would determine the barrier properties of the films.

Regarding permeability to oxygen and carbon dioxide (Fig. 1b and c), CMC-extract films presented lower values than the CMC-water films. Oxygen permeability tended to decrease (without being significantly different) with the addition of MMT to these formulations, while permeability to carbon dioxide increased in nanocomposite films with murta extract compared to CMC-water films. These differences reflect the differential solubility of different gases in presence or absence of the active compounds of the murta extract. The competition between the possible interactions: CMC–murta, CMC–clay or murta–clay, leads to the formation of materials with different polymer matrices, so that in these complex systems the differential solubility of water and gas molecules would be affecting permeability values. In this sense, Bifani et al. (2007) showed the same trend for permeability to O_2 (increased permeability for CMC-water films, and decreased permeability for CMC-extract ones), whereas trends in permeability to carbon dioxide with murta extract addition were not as consistent, obtaining in films of CMC-extract with higher amount of flavonols (M/Q = 12.84) a permeability value equivalent to 70% of that found for CMC-water films, and with the extract with lower flavonols content (M/Q = 10.15) a value equivalent to 54% of that of CMC-water films. In the present study (Fig. 1b), a permeability value equivalent to 28% was obtained with the use of extract of murta from the Casa ecotype (M/Q = 5.33). It seems that a different proportion of myricetin over quercetin may modulate the oxygen barrier property. In Fig. 1c, although the permeability to CO_2 was lower in CMC-films with extract than in those with water, the addition of MMT to the films resulted in an increased permeability to CO_2, which could suggest some selective action of these films to CO_2 permeability, with a possible higher solubility of CO_2 in the nanocomposite films with extract.

Therefore, selective barrier properties were observed for WVP according to the use of MMT, and for O_2 according to the use of murta extract or MMT. Results did not yield enough evidence for CO_2 permeability, in agreement with previous reports (Bifani et al., 2007), and indicate that this murta ecotype extract confers some barrier properties to CMC films when MMT is present.

The different selective barrier properties of these films would be important for different applications, e.g. in fruits with high respiration metabolism.

3.3. Mechanical properties

Fig. 2 shows the tensile mechanical properties measured in the films reinforced with MMT and/or activated extract of murta leaves. It shows that adding murta extract to the formulation seems to exert a plasticizing effect on the materials, reflected in a reduced tensile strength and modulus with a decrease in elongation at break. This plasticizing effect may also be associated to the observed increase in water absorption of these materials not accompanied by an increase in water vapor permeability. Gomez-Guillén et al. (2007) also observed a decrease in the puncture resistance of gelatin films using murta extract as solvent.

In turn, when either water or murta extract were used as solvent, increasing concentrations of clay in the formulation significantly increased the tensile strength and Young's modulus at the expense of elongation at break. For example, films with addition of

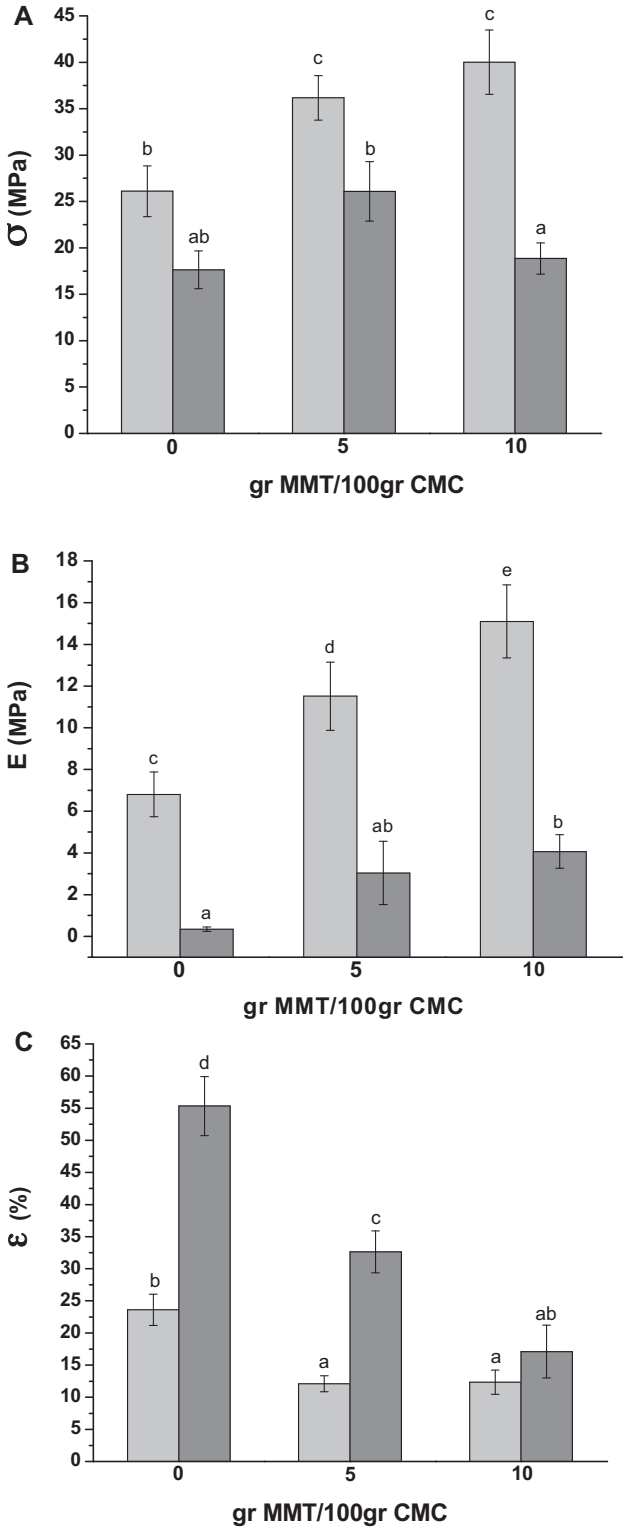

Fig. 2. Mechanical properties of CMC films with different contents of MMT obtained from film forming dispersion using water ( ) and murta leaves' extract ( ) as solvent: A – Tensile strength (σ), B – Young Modulus (E) and C – Elongation at break (ε).

10 g MMT/100 g CMC obtained from aqueous dispersions improved their tensile strength by 54% and Young's modulus by 122%, respectively, compared to control films, and these values decreased 59% and 80% by replacing water with the extract of murta in the film forming dispersions.

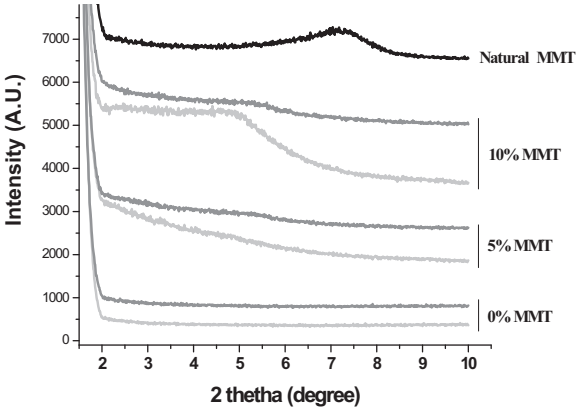

Fig. 3. XRD patterns of natural MMT powder and CMC–MMT films with ( ) and without ( ) murta leaves' extract.

Rimdusit et al. (2008) also improved the tensile strength and modulus of CMC films by the addition of montmorillonite. The enhancement of the modulus and the tensile strength can be directly attributed to the reinforcement provided by the high aspect ratio and the high surface area of silicate layers, to the good dispersion of clay layers in the CMC matrix, and to the strong interactions among them.

In the nanocomposite systems obtained from film forming dispersions using murta as solvent, there are two opposite effects – the plasticizing of CMC matrix by the compounds present in the extract of murta and its reinforcement by the clay, leading to intermediate mechanical behavior for these materials.

3.4. Nanocomposites structure

X-ray diffraction (XRD) studies were performed in order to analyze the dispersion grade of MMT platelets in CMC films. Fig. 3 depicts the XRD patterns of native MMT and CMC films with different MMT proportions, activated or not by murta leaves' extract. Whereas no characteristic peak was observed for CMC films (with or without murta compounds) in the XRD analyzed range, MMT exhibited a single 0 0 1 diffraction peak around 7.2°, which corresponds to an interlayer spacing, $d(0\,0\,1) = 1.2$ nm.

In general, the intercalation of the polymer chains between the clay interlayers usually increases the interlayer spacing, leading to a shift of the diffraction peak towards lower angle values (angle and layer spacing values being related through the Bragg's relation). As far as exfoliated structure is concerned, no more diffraction peaks are visible in the XRD patterns either because the space between the layers is much longer (i.e. exceeding 8 nm in the case of ordered exfoliated structure) or because the nanocomposite does not present an ordered structure (Alexandre & Dubois, 2000). The XRD pattern of nanocomposite films with 5 g MMT/100 g CMC obtained from aqueous dispersion is characteristic of systems where the clay is completely exfoliated, with disappearance of the characteristic peak of MMT without the appearance of any other peak; only a broadening or uprising of the base line is observed. The corresponding pattern of films with 10 g MMT/100 g CMC, in addition to presenting the uprising in the baseline, presented a shoulder at $2\theta = 4.9°$ (d-spacing = 1.8 nm), showing the formation of nanocomposite structure with intercalation of CMC chains in the gallery of the silicate layers of MMT, which causes increased spacing compared with that of the native MMT. At the same clay some platelets may be pushed apart and exfoliated, being distributed randomly in the CMC matrix.

The XRD patterns of nanocomposite formed from murta leaves' extract showed the same appearance, but for both concentrations of clay a shoulder at $2\theta = 5.34°$ ($d = 1.65$) appeared, being more marked the shoulder intensity at 10 g MMT/100 g CMC. It is clear that the presence of murta active compounds seems to result in a reduced spacing between the clay interlayers.

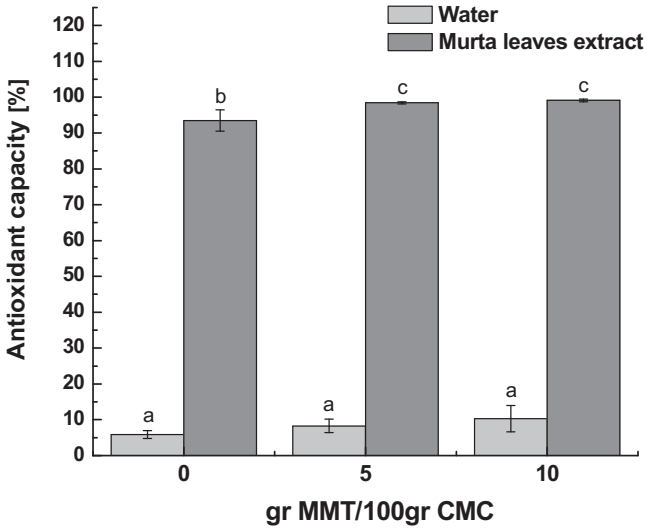

Fig. 4. Antioxidant capacity ($ABTS^{\bullet+}$ scavenging activity) of CMC films reinforced with MMT and/or activated with murta leaves' extract.

Chiou et al. (2007) and Tang et al. (2008) reported that increasing the concentration of glycerol (used as plasticizer) in MMT-starch films favored the formation of intercalated structures over the exfoliated ones. As in the XRD patterns of the present study, they observed the disappearance of the original peak of the nanoclay with the appearance of a new peak attributed to intercalated structures, which appears at higher 2θ values as the plasticizer concentration is increased. These authors concluded that incorporating sufficient glycerol into the starch–nanoclay samples inhibited intercalation to a certain extent because an increase in glycerol–starch interactions might compete with interactions between glycerol, starch, and the clay surface. The effect observed for glycerol in those previous studies could be compared with that produced by compounds present in the extract of murta. Further proofs in favor of this hypothesis are the characteristics of XRD patterns, as well as the observed plasticizing effect on mechanical properties and moisture content, and the changes observed in the barrier properties.

Regardless of the effect exerted by the murta extracts, the observed improvements in mechanical and barrier properties of the materials studied in this work can be correlated with the high degree of exfoliation/intercalation reached by the materials. And this can be attributed to the use of an appropriate procedure to disperse the clay, as well as the possible interactions between the clay and CMC that favored the intercalation of the CMC chains between silicate layers.

3.5. Antioxidant properties

Fig. 4 shows the antioxidant capacity (measured by the ABTS radical scavenging capacity) of the studied films. The antioxidant capacity of the films obtained using murta extract as solvent increased more than 18-fold compared to the CMC control film. The water extracts of murta leaves are rich in derivatives of gallic acid, myricetin and quercetin (Rubilar et al., 2006), and these compounds would be responsible for the antioxidant activity of the films studied. The addition of MMT to CMC–murta extract formulations resulted in a significant increase of the antioxidant activity, an effect not observed in the absence of the extract, where the basal

Table 2
Color parameters (L^*, a^*, b^* and ΔE) of films reinforced with montmorillonite and/or activated with murta leaves' extract.

Film	L^*	a^*	b^*	ΔE
With water				
0 g MMT/100 g MMT	92.13 ± 0.12^{b}	0.53 ± 0.01^{b}	1.79 ± 0.07^{a}	$5.18 \pm 0.12^{a,b}$
5 g MMT/100 g MMT	92.54 ± 0.07^{a}	0.41 ± 0.01^{c}	2.51 ± 0.03^{b}	4.84 ± 0.07^{a}
10 g MMT/100 g MMT	91.91 ± 0.23^{b}	0.15 ± 0.02^{d}	3.55 ± 0.21^{c}	5.70 ± 0.24^{b}
With murta extract				
0 g MMT/100 g MMT	81.88 ± 0.31^{c}	-2.59 ± 0.10^{f}	45.30 ± 0.53^{f}	46.32 ± 0.58^{d}
5 g MMT/100 g MMT	80.51 ± 0.33^{d}	-1.34 ± 0.06^{e}	44.50 ± 0.41^{e}	45.99 ± 0.49^{d}
10 g MMT/100 g MMT	78.19 ± 0.34^{e}	1.13 ± 0.07^{a}	42.74 ± 0.57^{d}	45.28 ± 0.63^{c}

Reported values for each films are means ± standard deviation. Values means by the same letter in column are not significantly different ($p < 0.05$) according to Tukey's test.

values, not significantly different among them, had only 6–10% of the antioxidant activity shown by samples containing murta extract. The low antioxidant activity shown by the films formed with water instead of extract can probably be explained by some interactions that could suffer the hydroxyl groups of the CMC with the ABTS$^{\bullet+}$ reagents of the method. Results shown in Fig. 4 would suggest that the active compounds of the extract present in the film presented a better availability in systems containing clay. This could be due to competition between the interactions of the reactive sites of the active compounds and the clay ones with the CMC, as mentioned above in the discussion of other properties studied.

Tunc et al. (2007) reported that aroma transfer properties could be modulated by the introduction of relatively low amounts of montmorillonites clays in the formulation of wheat gluten films, due to a different structuring of the protein network in the presence of layered silicates and an increased tortuosity, each reducing the aroma diffusivity. Ashby and Binks (2000) reported that layered silicates stabilized colloidal suspensions and emulsions by modifying interactions between oil and water phases and preventing coalescence due to their high surface/mass ratio and sorption capacity. These characteristics enabled nanoclays to function as potential "carriers" in controlled drug delivery system based on different polymer matrixes (Mascheroni et al., 2010).

It is planned to study more thoroughly the release of the active compounds of murta from their entrapment in CMC–MMT films, in order to assess whether these nanoreinforcements could modulate the release of active compounds and protect them during processing.

3.6. Appearance

Fig. 5 shows that by using the extract of murta as a solvent instead of water in the film forming dispersions, the color of the films changed, without significant differences in appearance by adding or increasing the concentration of montmorillonite in the formulation, although there are statistically significant differences in the color parameters (L^*, a^*, b^*, and ΔE), as it was shown in Table 2. Being water-based films colorless, CMC films with murta extract showed a yellowish-green color, corresponding to an increase of b^* and decrease of a^* and L^* parameters. Because of this slightly darker aspect of films due to the murta extract, their light barrier properties could change. Gomez-Guillén et al. (2007) compared the spectroscopic scanning of gelatin and gelatin-murta films and observed that at the beginning of the visible spectrum ($\lambda \cong 400$ nm) the film with antioxidant extracts presented an absorbance level approximately 6 times higher than the control gelatin film, being the differences in the ultraviolet spectrum even higher, and they suggested that films activated with murta extract could be an excellent barrier to prevent UV light-induced lipid oxidation, when applied to food systems.

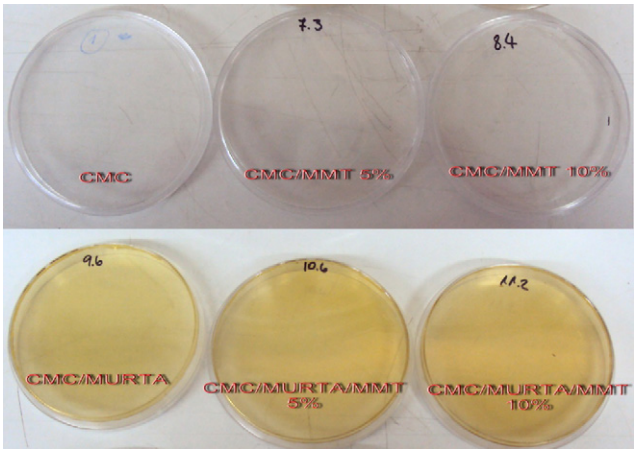

Fig. 5. Appearance of CMC, and CMC–MMT films activated or not with murta leaves' extract.

4. Conclusions

It was possible to improve the functionality of carboxymethylcellulose films reinforced with montmorillonite and to activate them with the polyphenols present in the extract of murta. The addition of MMT allowed to improve significantly the mechanical and barrier properties of films, due to the high degree of exfoliation/intercalation reached with the process used to obtain the materials and the possible interactions between CMC–MMT. Besides conferring important antioxidant properties, the use of the aqueous extract of murta as a solvent in film forming dispersions plasticized the CMC matrix and modified the ratio of permeability to different gases. Future studies will allow to determine whether the clays in these films can modulate the release of active ingredients.

Acknowledgements

The authors acknowledge ANPCyT-Project FONCyT-PICT 35036/05, UNLP-Project X-494 of Argentina, CYTED-Project 309AC0382, DIUFRO-Project 120617/DI06-0001 and INNOVA CORFO Project 06CN12PAT-57 of Chile for the financial support.

References

Alexandre, M. & Dubois, P. (2000). Polymer-layered silicate nanocomposites: Preparation, properties and uses of a new class of materials. *Material Science Engineering*, *28*, 1–63.

Almasi, H., Ghanbarzadeh, B. & Entezami, A. A. (2010). Physicochemical properties of starch–CMC–nanoclay biodegradable films. *International Journal of Biological Macromolecules*, *46*, 1–5.

Ashby, N. P. & Binks, B. P. (2000). Pickering emulsions stabilised by laponite clay particles. *Physical Chemistry Chemical Physics*, *2*, 5640–5646.

ASTM. (1989). Standard test methods for water vapor transmission of materials. Designation: E 96-80. In *Annual book of ASTM standards*. Philadelphia, PA: ASTM., pp. 745–754.

ASTM. (1991). Standard test methods for tensile properties of thin plastic sheeting. Designation: D882-91. In *Annual book of ASTM standards*. Philadelphia, PA: ASTM., pp. 182–190.

ASTM. (1994). Standard test methods for moisture content of paper and paperboard by oven drying. Designation D644-94. In *Annual book of ASTM standards*. Philadelphia, PA: ASTM., pp. 1–2.

Bifani, V., Ramírez, C., Ihl, M., Rubilar, M., García, A. & Zaritzky, N. (2007). Effects of murta (*Ugni molinae* Turcz) extract on gas and water vapor permeability of carboxymethylcellulose based edible films. *Lebensmittel wissenschaft und technologie*, *40*, 1473–1481.

Chiou, B., Wood, D., Yee, E., Imam, S. H., Glenn, G. M. & Orts, W. J. (2007). Extruded starch–nanoclay nanocomposites: Effects of glycerol and nanoclay concentration. *Polymer Engineering and Science*, *47*, 1898–1904.

Cyras, V. P., Manfredi, L. B., Ton-That, M. T. & Vazquez, A. (2008). Physical and mechanical properties of thermoplastic starch/montmorillonite nanocomposite films. *Carbohydrates Polymer*, *73*, 55–63.

Dean, K., Yu, L. & Wu, D. Y. (2007). Preparation and characterization of melt-extruded thermoplastic starch/clay nanocomposites. *Composites Science and Technology*, *67*, 413–421.

García, M. A., Martino, M. N. & Zaritzky, N. E. (2000). Lipid addition to improve barrier properties of edible starch-based films and coating. *Journal of Food Science*, *65*, 941–946.

Gennadios, A., McHugh, T. H., Weller, C. L. & Krochta, J. M. (1994). Edible coatings and film based on proteins. In J. M. Krochta, E. A. Baldwin, & M. Nisperos-Carriedo (Eds.), *Edible coatings and films to improve food quality* (pp. 201–278). Lancaster: Technomic Publishing Co., Inc.

Giannelis, E. P. (1996). Polymer-layered silicate nanocomposites. *Advanced Material*, *8*, 29–35.

Gómez Estaca, J., Giménez, B., Gómez-Guillén, C. & Montero, P. (2009). Incorporation of antioxidant borage extract into edible films based on sole skin or a commercial fish skin gelatin. *Journal of Food Engineering*, *92*, 78–85.

Gomez-Guillén, M. C., Ihl, M., Bifani, V., Silva, A. & Montero, P. (2007). Edible films made from tuna-fish gelatin with antioxidant extracts of two different murta ecotypes leaves (*Ugni molinae* Turcz). *Food Hydrocolloids*, *21*, 1133–1143.

Han, J. H. & Krochta, J. M. (2007). Physical properties of whey protein coating solutions and films containing antioxidants. *Journal of Food Science*, *72*, 308–314.

Huang, M. F., Yu, J. G. & Ma, X. F. (2004). Studies on the properties of montmorillonite-reinforced thermoplastic starch composites. *Polymer*, *45*, 7017–7023.

Karbowiak, T., Debeaufort, F., Champion, D. & Voilley, A. (2006). Wetting properties at the surface of iota-carrageenan-based edible films. *Journal of Colloid and Interface Science*, *294*, 400–410.

Mascheroni, E., Chalier, P., Gontard, N. & Gastaldi, E. (2010). Designing of a wheat gluten/montmorillonite based system as carvacrol carrier: Rheological and structural properties. *Food Hydrocolloids*, *24*, 406–413.

Montenegro, G. (2002). *Ugni molinae* Turcz. In G. Montenegro, & B. N. Timmermann (Eds.), *Chile nuestra flora útil. Guía de uso apícola, medicinal folclórica, artesanal y ornamental* (2nd ed., pp. 241–242). Santiago: Ediciones Universidad Católica de Chile.

Ogawa, M. & Kuroda, K. (1997). Preparation of inorganic–organic nanocomposites through intercalation of organoammonium ions into layered silicates. *Bulletin of the Chemical Society of Japan*, *70*, 2593–2618.

Rimdusit, S. J., Sorada, D., Siriporn, T. & Sunan, T. T. (2008). Biodegradability and property characterizations of MethylCellulose: Effect of nanocompositing and chemical crosslinking. *Carbohydrate Polymers*, *72*, 444–455.

Re, R., Pellegrini, N., Proteggente, A., Pannala, A., Yang, M. & Rice-Evans, C. (1999). Antioxidant activity applying an improved ABTS radical cation decolorization assay. *Free Radical Biology and Medicine*, *26*, 1231–1237.

Rubilar, M., Pinelo, M., Ihl, M., Scheuermann, E., Sineiro, J. & Nuñez, M. J. (2006). Murta leaves (*Ugni molinae* Turcz) as a source of antioxidant polyphenols. *Journal of Agricultural and Food Chemistry*, *54*, 59–64.

Seguel, I., Peñalosa, E., Gaete, N., Montenegro, A. & Torres, A. (2000). Colecta y caracterización molecular de germoplasma de murta (*Ugni molinae* Turcz.) en Chile. *Revista Agro Sur*, *28*, 32–41.

Sinha Ray, S. & Bousmina, M. (2005). Biodegradable polymers and their layered silicate nanocomposites: In greening the 21st century materials world. *Progress in Materials Science*, *50*, 962–1080.

Sinha Ray, S. & Okamoto, M. (2003). Polymer/layered silicate nanocomposites: A review from preparation to processing. *Progress in Polymer Science*, *28*, 1539–1641.

Tang, X., Alavi, S. & Herald, T. J. (2008). Effects of plasticizers on the structure and properties of starch–clay nanocomposite films. *Carbohydrate Polymers*, *74*, 552–558.

Tunc, S., Angellier, H., Cahyana, Y., Chalier, P., Gontard, N. & Gastaldi, E. (2007). Functional properties of wheat gluten/montmorillonite nanocomposite films processed by casting. *Journal of Membrane Science*, *289*, 159–168.